ELSEVIER

Contents lists available at ScienceDirect

Theoretical and Applied Fracture Mechanics

journal homepage: www.elsevier.com/locate/tafmec



On the mixed mode I/II/III translaminar fracture toughness of cotton/epoxy laminated composites



A. Zeinedini^{a,*}, M.H. Moradi^b, H. Taghibeigi^a, J. Jamali^c

- ^a Department of Mechanical Engineering, Kermanshah Branch, Islamic Azad University, Kermanshah, Iran
- ^b Department of Mechanical Engineering, Kermanshah University of Technology, Kermanshah, Iran
- ^c College of Engineering and Technology, American University of the Middle East, Kuwait

ARTICLE INFO

Keywords: Cotton/epoxy laminated composites Translaminar fracture Mixed mode I/II/III Critical strain energy release rate

ABSTRACT

The mixed mode I/II/III translaminar fracture of a natural fiber reinforced composites system was investigated in this paper. The specimens were made of epoxy resin and fabric cotton fibers. Compact shear tension (CTS) test configuration was utilized to determine a full range of mixed mode I/II/III translaminar critical strain energy release rate (CSERR). The CTS specimens were loaded by a novel test setup. In addition to pure modes I, II and III CSERR of cotton/epoxy system, a full series of mixed mode tests were conducted. Finite element analysis was also carried out to calculate the calibration factors related to the CSERR formulations. The pure mode I, II and III CSERR of cotton/epoxy laminates were obtained as 48.1, 57.8 and 1528.5 kJ/m², respectively. The investigation confirms that the translaminar CSERR of cotton/epoxy laminated composites is considerable as compared to the mode I translaminar CSERR of artificial fiber reinforced epoxy systems. Hence, due to this property and some other advantages such as biodegradability, biocompatibility and sustainability of the cotton/epoxy fiber laminated composites material can be a strong candidate to use in the place of different types of wood and synthesis fiber reinforced laminates.

1. Introduction

Natural fibers have been used in the fabrication of various products for many centuries due to their advantages such as high strength, renewability, recyclability, simple manufacturing process and low cost. In the recent years, the use of these fibers as reinforcement of polymerbased laminate composites has been considered. The application of natural laminated composites as a replacement of the wood and the artificial fiber reinforced laminated composites such as glass fiber reinforced plastic (GFRP), carbon fiber reinforced polymer (CFRP) and so on has been investigated and significant results have been obtained [1–4]. Composite sheets reinforced with the natural fibers are widely used in automotive, aviation, marine and construction industries. Under loading, different damage modes are occurred in the natural fiber laminated composites. The dominant failure modes in the laminated composites are inter-laminar and translaminar fracture [5-7]. Numerous investigations have been conducted on the inter-laminar fracture (delamination) in the natural and artificial fiber reinforcement laminated composites [5]. Literature review displayed that a few works have been performed on the translaminar fracture toughness (TFT) of natural fiber composites. While, some studies have been carried out to measure the translaminar fracture toughness of carbon/epoxy [8-16], glass/epoxy [17-24] and some other artificial [25,26] laminated composites. One of the first works on the translaminar fracture in carbon/epoxy laminated composites was published by Underwood and Kortschot [8]. Then, Gigliotti and Pinho [10] investigated the pure mode I translaminar fracture toughness of a carbon/epoxy composites system. The translaminar fracture response of carbon/epoxy laminates was studied by Laffan et al. [11]. They performed mixed mode I/II loading on cross-ply fiber reinforced specimens. Teixeira et al. [12] evaluated the effect of ply thickness on the mode I TFT of unidirectional carbon/epoxy laminated composites. It was concluded that by increasing the ply thickness from 0.03 to 0.12 mm, the TFT is enhanced from 46 to 104 kJ/m². The dependency of mode I TFT on the sample thickness of carbon/epoxy material was studied by Xu et al. [14]. The results manifested that as the specimen thickness varies between 1 and 8 mm, the mode I TFT is not significantly changed. Boyina et al. [18] studied the influence of fracture mode mixity on the TFT of woven glass fiber reinforced epoxy composites subjected to mixed mode I/II loading states. Arun et al. [20] explored the effect of particles, i.e. silicon carbide and graphite, on the mode I TFT of glass/epoxy laminates system. The results manifested that in the presence of graphite powder, the

E-mail address: zeinedini@iauksh.ac.ir (A. Zeinedini).

^{*} Corresponding author.

Table 1Mechanical and physical properties of the cotton fiber reinforced laminated composites.

Property	Value
Tensile stiffness, E_{11} (GPa)	4.00
Flexural stiffness, E_{fx} (GPa)	3.80
In-plane shear stiffness, G_{12} (GPa)	3.39
Tensile strength, S_T (MPa)	73.98
Flexural strength, S_B (MPa)	114.63
Shear strength, S_S (MPa)	45.60
Density, ρ (kg/m ³)	1126

mode I TFT of laminated composites is greater than the samples consisting of silicon carbide particles. Hou and Hong [24] studied the mode I TFT of a glass/epoxy system. The resistance curve (R-curve) of the system was obtained using digital image correlation. Syed Abdullah et al. [25] determined the TFT of Vectran/epoxy laminates under pure mode I loading conditions. The mode I TFT of Vectran/epoxy is remarkably higher than the TFT of carbon and glass fibers reinforced laminated composites. Liu et al. [26] explored the mode I TFT of woven

flax fiber reinforced epoxy laminated composites. These researchers evaluated the effect of the reinforcement architecture and its volume fraction on the TFT. It was found that TFT is dominated by the flax fiber volume fraction, rather than its architecture.

Various test configurations have been proposed to determine the translaminar fracture toughness of laminated composites [27]. To measure the mode I TFT, ASTM E1922 [28] is usually utilized. A modified version of Compact Tension (CT) sample was used by Syed Abdullah et al. [25] to characterize the mode I TFT. In order to study the fracture behaviors under shear-opening crack condition, different mixed mode fracture specimens were suggested [7]. Laffan et al. [11] and Jamali et al. [19] utilized a mixed mode CT specimen to obtain the TFT of the laminated composites under mixed mode I/II loading states. Boyina et al. [18] presented a modified CT sample loaded by an Arcan fixture for calculating the mixed mode I/II TFT. Recently, a novel fixture [29] was proposed to measure the mixed mode I/II/III fracture properties of brittle materials.

To the best knowledge of the authors, no research has been published on the mixed mode I/II/III translaminar fracture toughness of natural fiber reinforced laminated composites. Therefore, the translaminar fracture toughness of a cotton/epoxy laminated composites

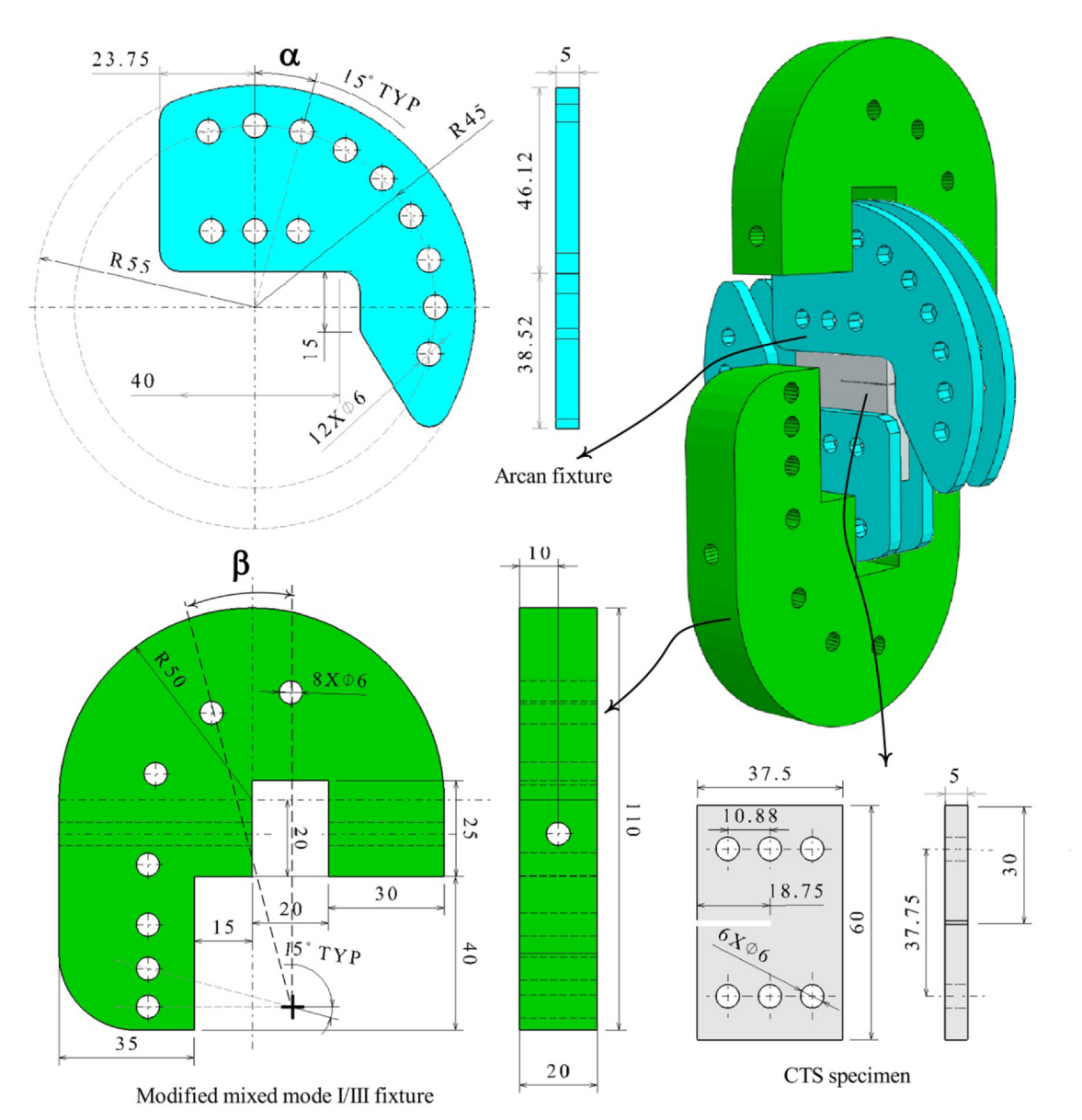


Fig. 1. The 3D fixture and the samples used to measure the translaminar fracture toughness of cotton/fiber laminated composites (all dimensions are in mm).

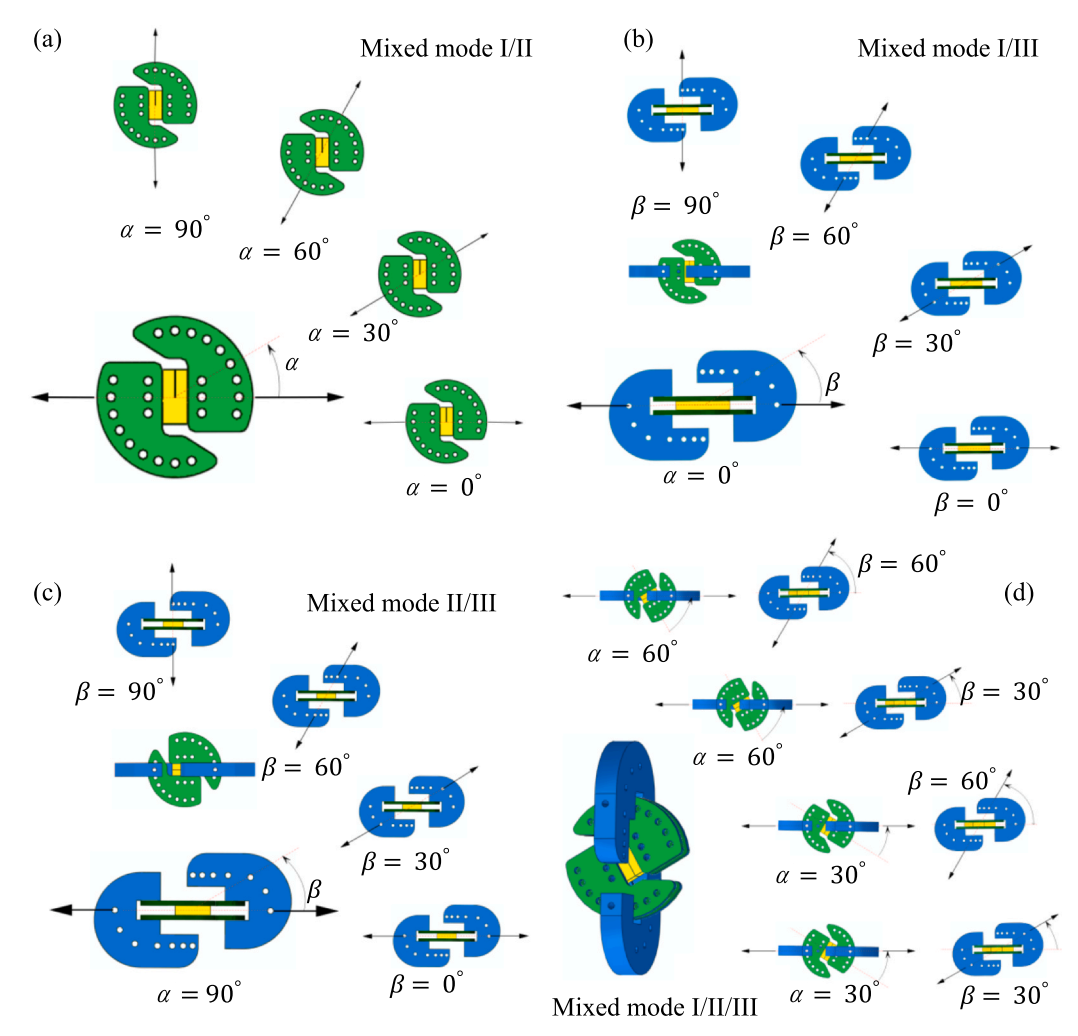


Fig. 2. The CTS specimen tested under (a) mixed mode I/II, (b) mixed mode I/III, (c) mixed mode II/III and (d) mixed mode I/II/III loading conditions.

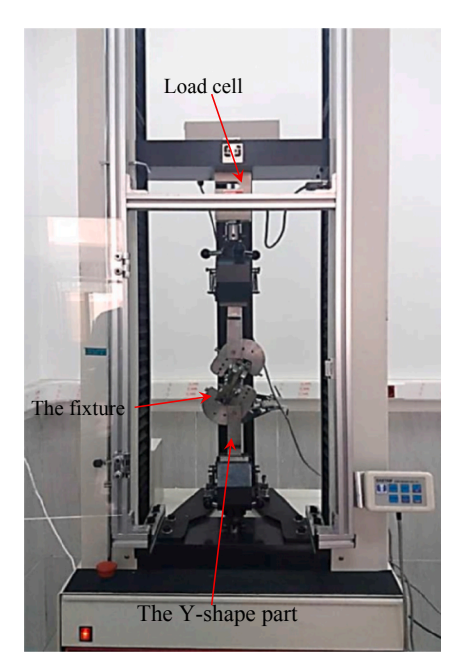


Fig. 3. The requirement setup for measuring the translaminar fracture toughness of the cotton/epoxy laminated composites samples.

system was investigated. A full range of mixed mode I/II/III loading conditions was regarded to apply on the cotton reinforced epoxy system. The CTS sample, a version of Arcan fixture and an out-of-plane fixture proposed by Zeinedini [29] was used to obtain the laminated composites response under various loading states. At the end, the mixed mode I/II/III TFT of the cotton/epoxy laminates was computed using the experimental results and a finite element analysis. The results obtained in this investigation are used to predict the out-of-plane crack growth initiation in the sheets made of cotton/epoxy laminates under any loading condition.

2. Experimental study

2.1. Specimen preparation

2.1.1. Materials selection

In the current research, the matrix of laminated composites has been considered to be consisted of an epoxy resin (LY5052) with a density of $1.11~{\rm g/cm}^3$ and a hardener (HY 5052) with the mixing ratio of 100:38. These materials were supplied by Momentive Specialty Chemicals, Inc. (Ohio, U.S.). Besides, plain weave fabric cotton fiber with the surface density of $171~{\rm g/m}^2$ was chosen as the reinforcement.

2.1.2. Mechanical properties

In order to compute the translaminar fracture toughness, the elastic properties of the samples must be determined at the first step. Furthermore, based on ASTM D3039 [30], ASTM D3518 [31], ASTM

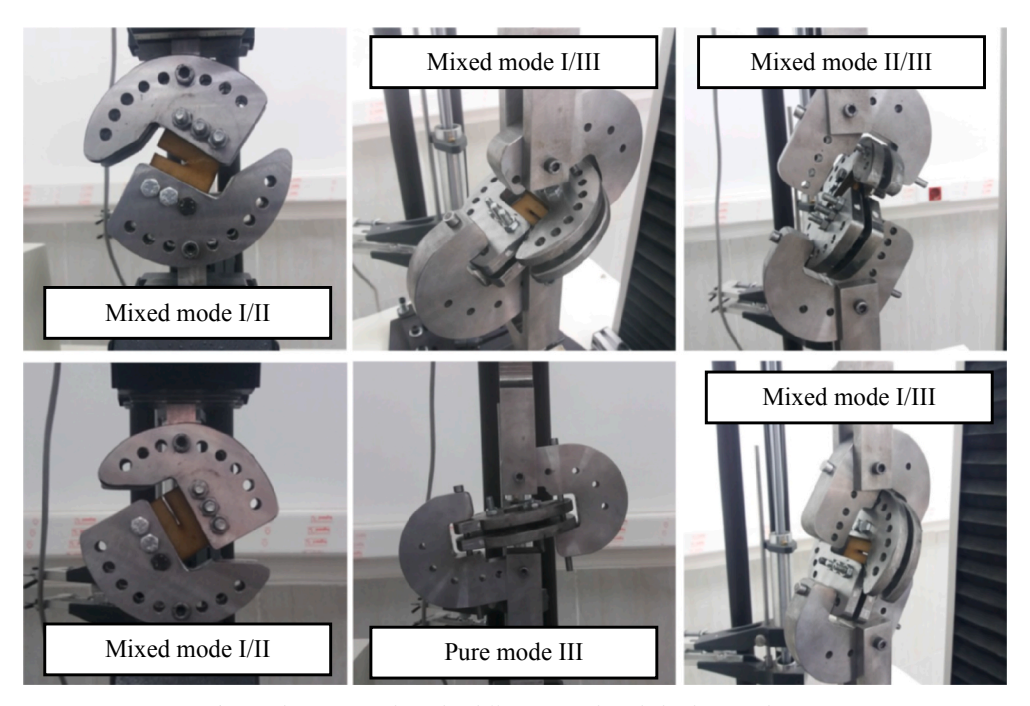


Fig. 4. The CTS sample under different mixed mode loading conditions.

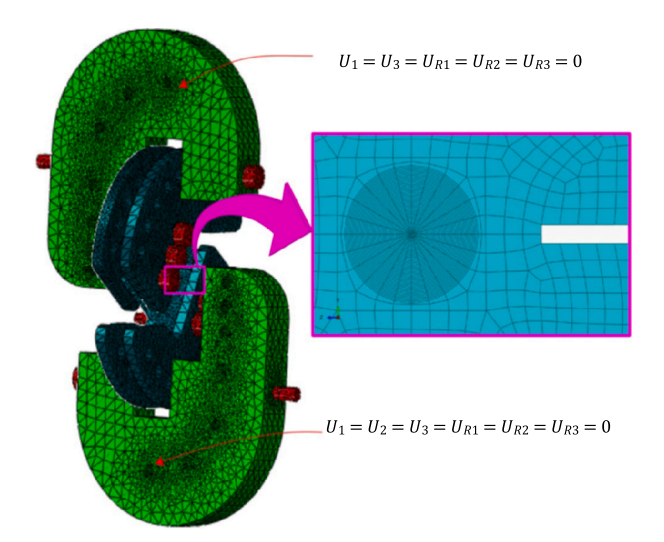


Fig. 5. The simulated fixture and CTS specimen. The displacement (U_i) and rotation (U_{Ri}) boundary conditions have been shown.

D790 [32], tensile, shear and flexural testing were done, respectively. The samples dimensions and the loading conditions were considered according to the corresponding standards. The mechanical properties of the cotton/epoxy system have been tabulated in Table 1.

2.1.3. Fracture samples

A plate consisting of 12 cotton/epoxy plies was manufactured by hand lay-up method. Some investigators [8] have evaluated the effect of sample thickness on the translaminar fracture toughness of laminated composites. It was proved that specimen thickness has not significant influence on the translaminar fracture toughness. Since small thickness of CTS sample may cause out-of-plane buckling [28], the thickness of CTS samples was considered as 5 mm. Some other researchers [11,18] considered the same values (see Fig. 1) for measuring the TFT of different materials. The specimens with the dimensions of 60 mm \times 37.5 mm \times 5 mm were cut from the manufactured plate by a laser machine. The sample dimensions were selected according to Ref.

[29]. Moreover, a through thickness notch of 2 mm span was cut. Finally, a sharp razor blade was used to create a pre-crack length of 1 mm at the notch tip [18].

2.2. Test procedure

As mentioned, in this study, the test configuration proposed by Zeinedini [29] was applied to determine the mixed mode I/II/III translaminar fracture toughness of cotton/epoxy laminated composites (see Fig. 1). As observed in Fig. 2, in addition to pure modes I, II and III, the CTS samples were loaded under mixed mode I/II loading conditions with in-plane loading angles (α) of 30° and 60°, mixed mode I/III and II/III loading rates with out-of-plane loading angles (β) of 30° and 60°. Under mixed modes I/III and II/III loading conditions α should be 0° and 90°, respectively. At the end, to observe the effect of mode mixity on the translaminar fracture behavior of the cotton/epoxy system, the samples were loaded under two mixed mode I/II/III loading conditions with loading angles of $\alpha=30$ ° and $\beta=60$ ° and $\alpha=60$ ° and

The experiment setup used to measure the translaminar fracture toughness of the cotton/epoxy samples has been displayed in Fig. 3. A universal testing machine (Santam STM-20) was utilized for testing the samples under displacement control condition. In addition, quasi-static condition was ensured by a crosshead speed of 0.25 mm/min. For recording the load, a load cell with the capacity of 20,000 N was used. The load (P) versus the displacement (δ) curves obtained by the Santam machine were the primary results. Some of the samples tested under a certain loading condition have been represented in Fig. 4.

3. Fracture properties calculation

The lack of any data reduction method for computing the translaminar CSERR or TFT of the CTS sample required that a finite element (FE) analysis be carried out. According to Refs. [11,12,25], in order to calculate the translaminar CSERR under any loading condition, a compliance calibration curve can be illustrated. Based on this method, a specimen with the thickness of 1 mm subjected to an applied load of $P=1\ N$ must be simulated as shown in Fig. 5. Hence, the CTS sample

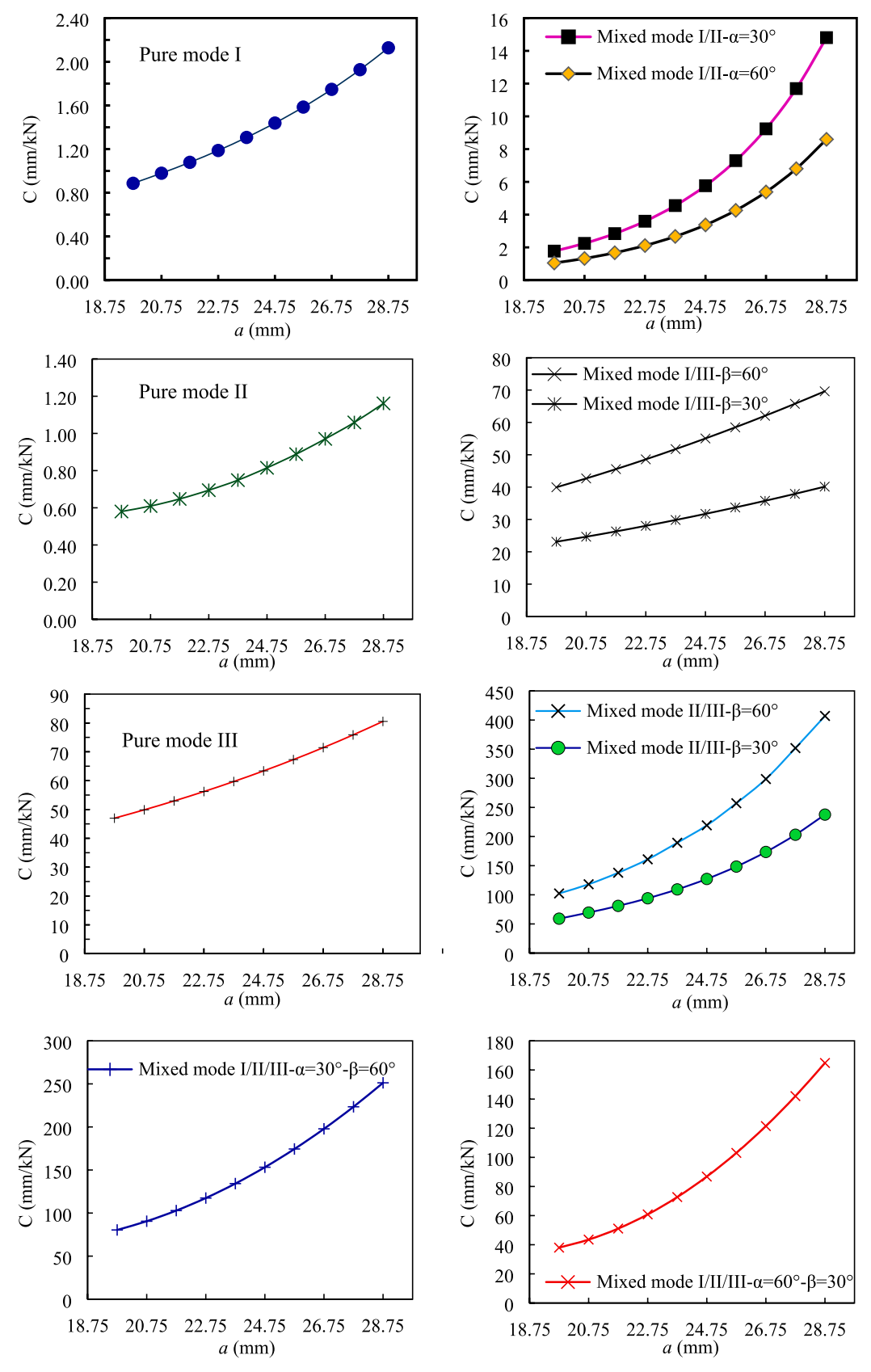
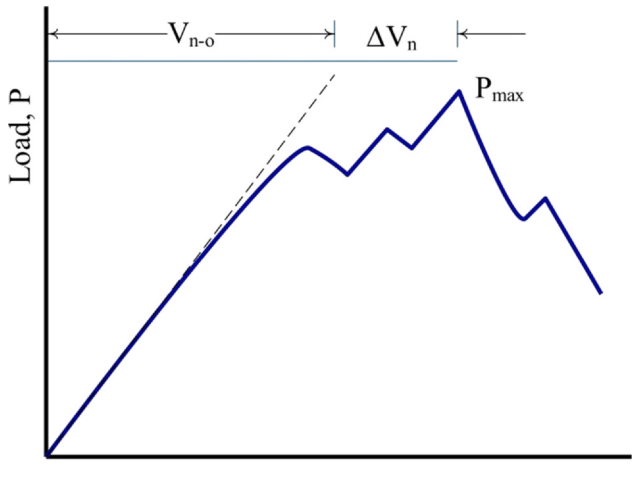


Fig. 6. The compliance calibration curves for different fracture modes obtained using finite element modeling.



Displacement

Fig. 7. The parameters in the load-displacement curves used to compute the upper bound value of translaminar CSERR.

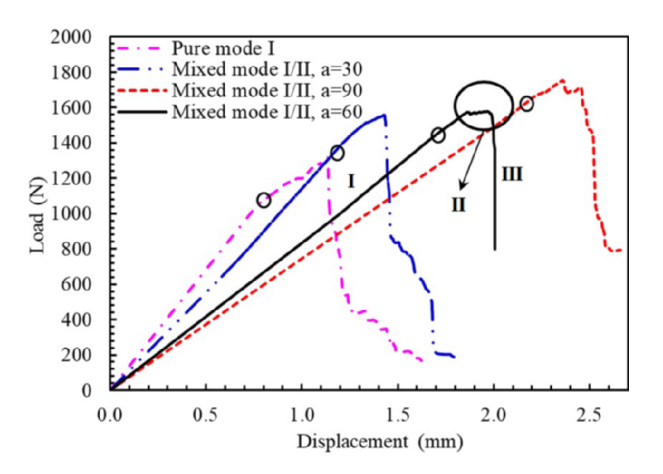


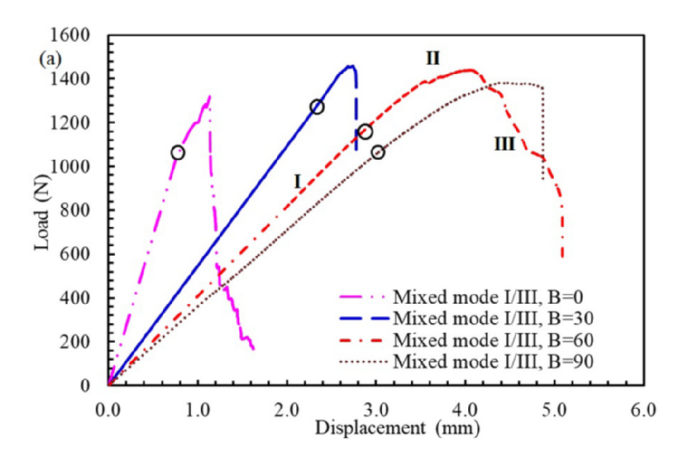
Fig. 8. The influence of in-plane loading angle (α) on the representative load vs displacement curves obtained from the testing of CTS samples as $\beta=0^\circ$. The circles represent the first non-linear load points.

and the fixture were simulated in ABAQUS/standard software. Based on Modified Compliance Calibration (MCC) method [11,12,25], in order to calculate the translaminar CSERR of each loading condition, many different simulations with ten crack lengths were performed. Contact between the CTS specimen, Arcan fixture, novel fixture and connecting pins were presumed to be frictionless. The specimen was gripped in the simulated fixture by pins similar to the experimental study. The boundary conditions have been also considered based on the practical work. The CTS sample was meshed using a total number of 17,230 C3D20R solid elements. As shown in Fig. 5, the elements were refined around the pre-crack tip of CTS specimen. It must be mentioned that the smallest mesh size was regarded as 0.1 mm in this region.

As displayed in Fig. 6, a compliance-crack length curve for each loading conditions can be plotted through the FE analysis. According to MCC method [11,12,25], a relation can be derived for each compliance calibration curve by fitting a function as follows:

$$C = \gamma e^{\delta a} \tag{1}$$

Where γ and δ can be determined to best fit the primary results. In addition, t is the CTS sample thickness and a is its crack length. The translaminar CSERR of laminated composites tested under a certain loading condition can be determined as follows [11]:



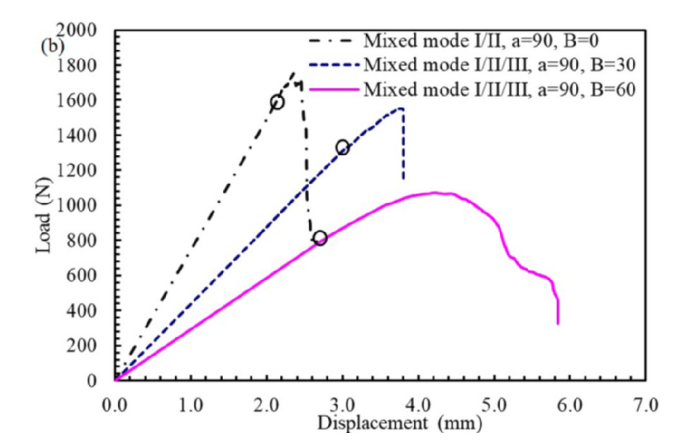


Fig. 9. The effect of out-of-plane loading angle (β) on the representative load vs displacement curves obtained from testing of the CTS samples as (a) $\alpha = 0^{\circ}$ and (b) $\alpha = 90^{\circ}$. The circles represent the first non-linear load points.

$$G_{c} = \frac{P_{c}^{2}}{2t} \frac{dC}{da} \tag{2}$$

where C and P_c are the compliance and the critical load of the system under a specific loading conditions, respectively. Finally, the translaminar CSERR of laminated composites can be computed by replacing Eq. (1) into Eq. (2) as:

$$G_{c} = \frac{P_{c}^{2}}{2t} \gamma \delta e^{\delta a} \bigg|_{a=a_{0}} \tag{3}$$

where a_0 is the crack length and it is equal to 19.75 mm in this study. The change of compliance of the simulated cotton/epoxy system under different loading conditions versus the crack length has been displayed in Fig. 6. According to the FE analysis, the compliance of system under mixed mode II/III loading condition is greater than the other fracture modes at a certain crack length.

The mode I, II and III translaminar strain intensity factor for a transverse isotropic material with the crack line parallel to the principal direction is determined from the following equation [25,33,34]:

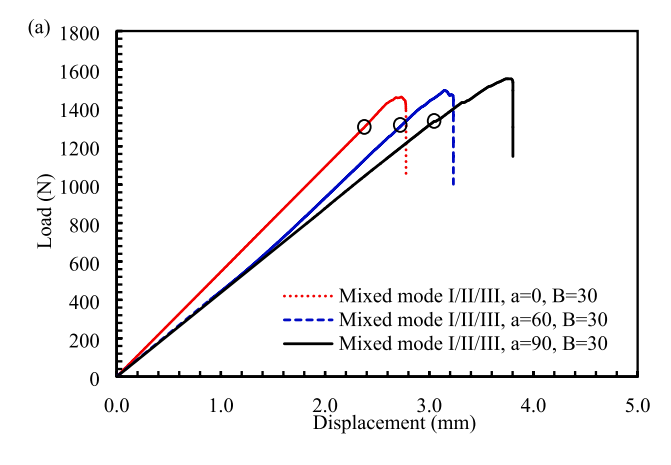
$$K_I = \sqrt{G_I E_I} \tag{4}$$

$$K_{II} = \sqrt{G_{II}E_{II}} \tag{5}$$

$$K_{III} = \sqrt{2G_{III}\mu} \tag{6}$$

where E_I and E_{II} are the effective tensile moduli and μ is the shear stiffness of the system. For transverse isotropic plates under generalized plane stress conditions, E_I , E_{II} and μ are defined as [33,34]:

$$E_I = \sqrt{2/(a_{11}a_{22})} / \sqrt{a_{22}/a_{11}} + \{(2a_{12} + a_{66})/(2a_{11})\}$$
 (7)



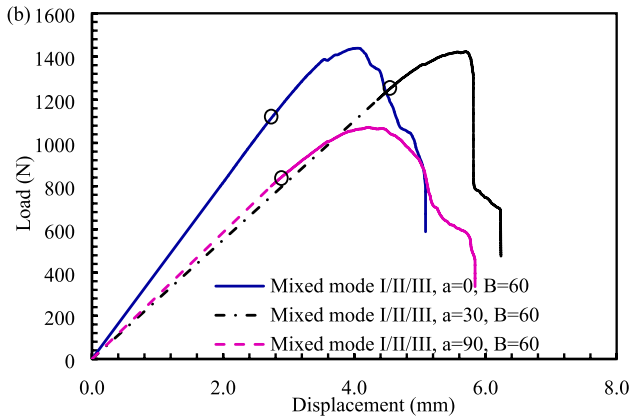


Fig. 10. The influence of in-plane loading angle (α) on the representative load vs displacement curves obtained from testing of the CTS samples as (a) $\beta = 30^{\circ}$ and (b) $\beta = 60^{\circ}$. The circles represent the first non-linear load points.

$$E_{II} = (\sqrt{2}/a_{11})/\sqrt{\sqrt{a_{22}/a_{11}} + \{(2a_{12} + a_{66})/(2a_{11})\}}$$
(8)

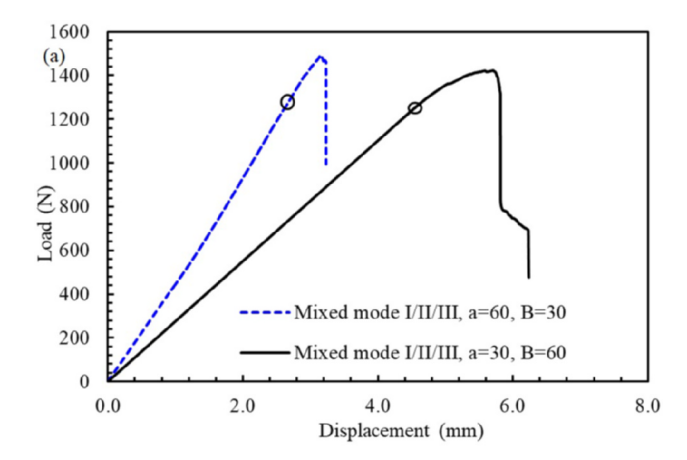
$$\mu = 2/(a_{55} + a_{66}) \tag{9}$$

where a_{ij} are expressed in terms of the following engineering elastic constants of the laminate [35]:

$$\begin{split} a_{11} &= \frac{1}{E_x}, \quad a_{22} &= \frac{1}{E_y}, \quad a_{33} &= \frac{1}{E_z}, \quad a_{44} &= \frac{1}{G_{yz}}, \quad a_{55} &= \frac{1}{G_{xz}}, \quad a_{66} &= \frac{1}{G_{xy}}, \\ a_{12} &= a_{21} &= -\frac{v_{xy}}{E_x} &= -\frac{v_{yx}}{E_y}, \quad a_{13} &= a_{31} &= -\frac{v_{xz}}{E_x} &= -\frac{v_{zx}}{E_z}, \\ a_{23} &= a_{32} &= -\frac{v_{yz}}{E_y} &= -\frac{v_{zy}}{E_z}, \end{split}$$

According to the references related to the fracture mechanics of laminated composites in the presence of fiber bridging phenomenon [28,36-39], three points, i.e., deviation from linearity (NL), Visual Observation (VIS) and Maximum Load, can be assumed as the critical load point which the crack initiates to growth. The first critical load value for determining the fracture toughness can be considered from the load-displacement curve at the point of deviation from linearity, or onset of nonlinearity (NL). It can be stated that the NL value represents a lower bound value for the fracture toughness. For brittle matrix composite materials, this is typically the same point at which the crack growth initiation is observed [36,40]. In addition to the load-displacement curves, since the crack deflection in the cotton/epoxy CTS samples is similar to the brittle fracture in materials such as pure epoxy [29], it is concluded that the translaminar fracture in cotton/epoxy system has brittle behavoiur. Thus, the NL value can be considered as one of the point related to the crack growth initiation and can be used to calculate the translaminar fracture toughness.

Because of the structure of test fixture, the Visual Observation



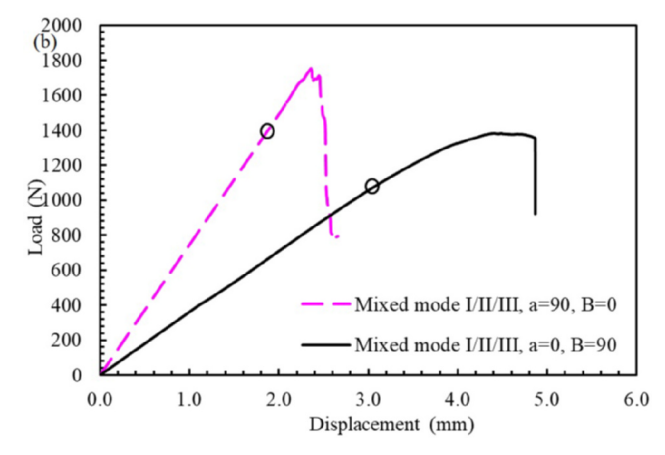


Fig. 11. The effect of changing the loading angle from the in-plane condition to out-of-plane when (a) α , $\beta=30$ or 60° and (b) α , $\beta=0$ or 90° . The circles represent the first non-linear load points.

cannot be applied to compute the CSERR.

In the other side, regarding this comment, the upper bound value of translaminar fracture toughness was also determined according to ASTM E1922 [28]. Even though this standard was presented for the pure mode I loading condition, it was used to the other loading condition in the current study. Based on this standard, to compute the translaminar fracture toughness, the following procedure must be used:

- Determine the maximum applied G value as G_{max} , which corresponds to the maximum load during the test, P_{max} .
- Determine the deviation from the linear trend fraction ($\Delta V_n/V_{n-o}$) by obtaining the values of ΔV_n and V_{n-o} from the load versus displacement plot, using the procedure shown in Fig. 7.
- If $\Delta V_{\rm n}/V_{\rm n-o} \leq 0.3,$ then the upper bound value can be computed using this method.

4. Results and discussion

Representative load–displacement curves for each mixed mode I/II/ III translaminar fracture test have been shown in Figs. 8–11. It is demonstrated that for some of the load–displacement curves, three regions can be considered (see Fig. 8). In the region I, the load is linearly increased versus the load point displacement until the first nonlinear point. This response is observed for all the tested specimens. In the region II, the load–displacement curve becomes non-linear. This region is related to the crack propagation. Similar behavior was observed by the other researchers [11,18]. It is observed that the curve has ascending behavior between the first nonlinear and the maximum load points. After the peak load, the load drops rapidly. It means that the

(10)

Table 2
The fitting parameters for different loading conditions defined in Eq. (1) and obtained from the FE analysis, the NL load and the related CSERR (the lower bound value)of the cotton/epoxy system under different loading states.

Loading condition	γ	δ	P_{NL} (N)	G_{C-NL} (kJ/m ²)
Pure mode I	0.1309	0.0969	1059.2 ± 46.7	48.1 ± 0.093
Mixed mode I/II, $\alpha = 30^{\circ}$	0.0192	0.2303	1355.3 ± 70.2	380.9 ± 1.022
Mixed mode I/II, $\alpha = 60^{\circ}$	0.0203	0.2129	1454.8 ± 68.0	304.4 ± 0.665
Pure mode II	0.1009	0.0839	1616.4 ± 45.1	57.8 ± 0.045
Mixed mode I/III, $\alpha = 30^{\circ}$	6.9089	0.0614	1270.8 ± 67.0	1149.5 ± 3.195
Mixed mode I/III, $\alpha = 60^{\circ}$	11.885	0.0617	1094.6 ± 28.3	1483.0 ± 0.991
Pure mode III	13.702	0.0618	1033.1 ± 42.3	1528.5 ± 2.562
Mixed mode II/III, $\alpha = 90^{\circ}$, $\beta = 30^{\circ}$	2.8431	0.1538	1301.3 ± 55.2	7683.9 ± 13.826
Mixed mode II/III, $\alpha = 90^{\circ}$, $\beta = 60^{\circ}$	4.8081	0.1545	870.1 ± 29.1	5917.2 ± 6.619
Mixed mode II/III, $\alpha = 30^{\circ}$, $\beta = 60^{\circ}$	6.3574	0.1283	1272.8 ± 63.5	8293.4 ± 20.642
Mixed mode II/III, $\alpha = 60^{\circ}$, $\beta = 30^{\circ}$	1.3738	0.1671	1264.0 ± 50.2	4947.4 ± 7.803

Table 3 The deviation fraction ($\Delta V_n/V_{n-o}$) defined in section 3 and obtained from the load–displacement curve for different loading conditions. The maximum load and the related CSERR (the upper bound value) of the cotton/epoxy system under different loading states.

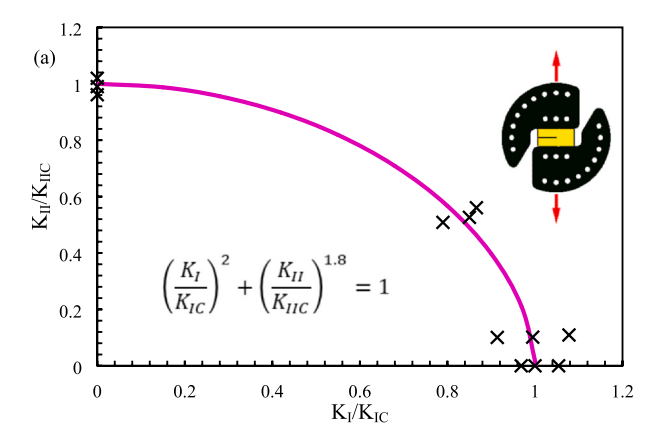
Loading condition	$\Delta V_n/V_{n-o}$	P_{MAX} (N)	$G_{C\text{-}MAX}$ (kJ/m ²)
Pure mode I	0.16	1312 ± 63.4	73.78 ± 0.17
Mixed mode I/II, $\alpha = 30^{\circ}$	0.12	1536 ± 74.9	489.32 ± 1.16
Mixed mode I/II, $\alpha = 60^{\circ}$	0.08	1548 ± 84.3	344.68 ± 1.02
Pure mode II	0.04	1725 ± 70.5	65.87 ± 0.11
Mixed mode I/III, $\alpha = 30^{\circ}$	0.04	1460 ± 67.0	1517.29 ± 3.19
Mixed mode I/III, $\alpha = 60^{\circ}$	0.21	1441 ± 41.5	2570.21 ± 2.13
Pure mode III	0.15	1377 ± 58.2	2715.52 ± 4.85
Mixed mode II/III, $\alpha = 90^{\circ}$, $\beta = 30^{\circ}$	0.06	1554 ± 75.3	10958.00 ± 25.73
Mixed mode II/III, $\alpha = 90^{\circ}$, $\beta = 60^{\circ}$	0.14	1075 ± 32.6	9032.23 ± 8.31
Mixed mode II/III, $\alpha = 30^{\circ}$, $\beta = 60^{\circ}$	0.11	1420 ± 69.1	10322.6 ± 24.44
Mixed mode II/III, $\alpha = 60^{\circ}$, $\beta = 30^{\circ}$	0.03	1478 ± 63.8	6764.39 ± 12.60

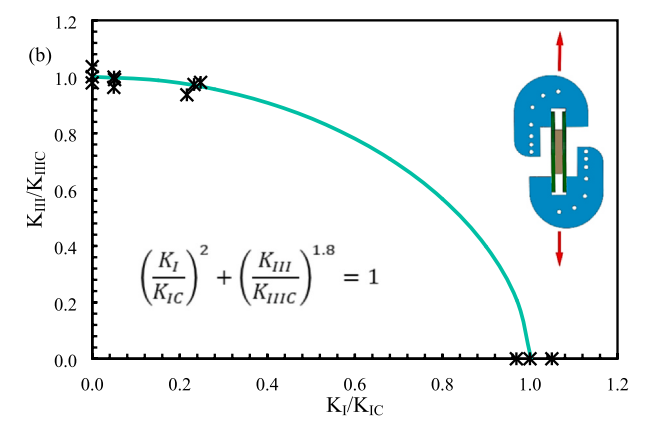
Table 4The effective moduli and translaminar fracture toughness of cotton/epoxy system under various loading states.

Loading condition	E_I (GPa)	E_{II} (GPa)	μ (GPa)	K_{C-NL} (MPa \sqrt{m})	$K_{C\text{-}MAX}$ (MPa \sqrt{m})
Mode I	4.1	_	_	14.05	17.40
Mode II	_	4.1	-	15.41	16.44
Mode III	-	-	2.0	78.19	104.22

crack propagation has an unstable behavior like brittle material. For the other loading conditions, a distinctive behavior was revealed. For these plots, three regions can be also considered as displayed in Fig. 9a. It is shown that these regions are; (I) linear behavior, (II) a non-linear response up to the peak load and (III) a steady state crack propagation. The steady state crack propagation can be induced by the fiber-bridging phenomenon [25].

In addition, the effect of in-plane and out-of-plane loading angles on the load–displacement curves can be exhibited in Figs. 8–11. Fig. 8 displays the influence of in-plane loading angle (α) on the load vs displacement curves of CTS samples tested under mixed mode I/II loading conditions. It is clear that the loading condition (mode mixity) has a significant effect on the translaminar fracture response of the cotton/epoxy laminates. Similar behavior was also reported by Laffan et al. [11] and Boyina et al. [18] for carbon/epoxy and glass/epoxy material systems, respectively. Fig. 9a and b shows the influence of out-of-plane loading angle (β) value on the translaminar fracture response of cotton/epoxy system when α is equal to 0° and 90°, respectively. In





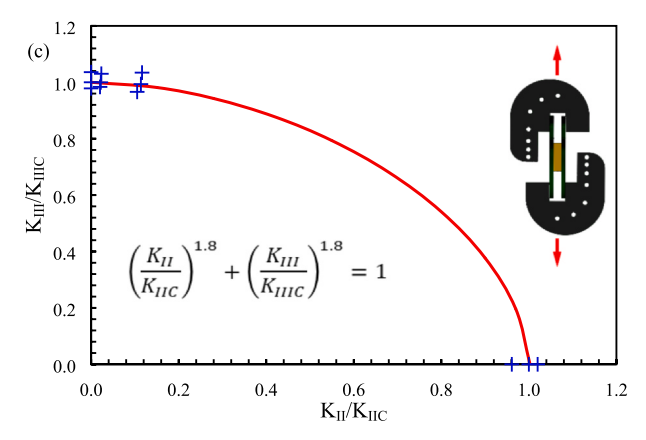


Fig. 12. The translaminar fracture envelopes obtained for the cotton fiber reinforced composites under (a) mixed mode I/II, (b) mixed mode I/III and (c) mixed mode II/III loading conditions.

Table 5
The comparison of the translaminar CSERR of cotton/epoxy material with some other systems.

Material	G_{IC-NL} (kJ/m ²)	Reference	$K_{IC\text{-}NL}$ (MPa/ \sqrt{m})	Reference
Woven cotton/epoxy	48.1	Present work	14.05	Present work
Pure epoxy	0.192-0.212	Supplier data sheet	0.77-0.83	Supplier data sheet
Woven carbon/epoxy	28.9	[37]	_	_
Woven glass/epoxy	50.0	[18]	_	_
Unidirectional carbon/epoxy with a stacking sequence of [904/0/904] _{2S}	95.50	[11]	_	-
Unidirectional carbon/epoxy	91.6	[35]	_	_
Unidirectional carbon/epoxy	56.1	[38]	_	_
Unidirectional carbon/epoxy	97.8	[39]	-	-

Table 6Comparison of interlaminar and translaminar CSERR of the cotton/epoxy system under different loading states.

Loading condition	Translaminar CSERR (kJ/m²)	Inter-laminar CSERR (kJ/m²)
Pure mode I	48.1	0.127
Mixed mode I/II, $\alpha = 30^{\circ}$	380.9	0.145
Mixed mode I/II, $\alpha = 60^{\circ}$	304.4	0.213
Pure mode II	57.8	0.430
Mixed mode I/III, $\alpha = 30^{\circ}$	1149.5	0.165
Mixed mode I/III, $\alpha = 60^{\circ}$	1483.0	0.238
Pure mode III	1528.5	0.818
Mixed mode II/III, $\alpha = 90^{\circ}$, $\beta = 30^{\circ}$	7683.9	0.719
Mixed mode II/III, $\alpha = 90^{\circ}$, $\beta = 60^{\circ}$	5917.2	0.843

Fig. 9a, it is observed that by increasing the out-of-plane loading angle or the mode III fracture contribution, the slope of linear response (region I) of the curve drops. In other words the stiffness of the cotton/ epoxy system consisting of a notch decreases as the contribution of mode III translaminar fracture is enhanced. In Fig. 9b, it is well observed that as $\alpha = 90^{\circ}$, the response of cotton/epoxy laminated composites is strongly dependent on the out-of-plane loading angle. Fig. 10a displays the effect of in-plane loading angle on the load-displacement curve of the cotton/epoxy laminated composites as $\beta = 30^{\circ}$. As a result, the in-plane loading angle has negligible effect on the non-linear load point of the system. However, by increasing the in-plane loading angle (the mode II contribution), the slope of linear elastic region of the sample is decreased. Also in Fig. 10b, representative load-displacement curves for the cotton/epoxy system tested under mixed mode I/II/III loading condition as $\beta = 60^{\circ}$ and α changed from 0 to 90° were shown. It is observed that the effect of the in-plane loading on the material response is not significant. The influence of changing the loading angle from in-plane to the out-of-plane state is shown in Fig. 11a and b. It can be concluded that by changing the loading angle condition from inplane to out-of-plane and vice versa, the behavior of material is clearly changed as depicted in Fig. 11a and b. In the other words, the parameters such as the linear region slope, the first nonlinear and peak loads, and the steady state crack propagation are significantly affected by the loading angle condition.

4.1. CSERR results

The results obtained for the lower and upper bound values of translaminar CSERR of cotton/epoxy system under different loading conditions have been listed in Tables 2 and 3, respectively. It must be mentioned that the fraction of $\Delta V_{\rm n}/V_{\rm n-o}$ is smaller than 0.3 for all loading condition (see Table 3); therefore the translaminar fracture toughness under any loading condition can be determined using the procedure explained in Section 3. It is well observed that for a certain loading condition, there is a considerable difference between the lower and upper bound values of translaminar CSERR. The measured values

of CSERR for pure mode II and mixed mode I/II translaminar fracture are more than pure mode I CSERR. This difference can be originated from fiber pull-out, fiber breakage, fiber—matrix debonding and matrix cracking. It is demonstrated in the next section that the damaged area under mode III loading condition to be much greater than that under mode I loading condition. It was also observed by Boyina et al. [18] that under pure mode I loading condition, the extent of fiber—matrix debonding as well as fiber pull-out is remarkably lesser in comparison with mode II loading condition. On the other hand, under out-of-plane loading condition (in the presence of mode III fracture), a non-linear behavior was observed in the load—displacement curves owing to the progressive energy dissipation using matrix cracking and fiber—matrix debonding mechanisms before unsteady final failure.

4.2. Translaminar fracture toughness

Using Eqs. (4)–(6) and Tables 2 and 3, the lower and upper bound values of mode I, II and III translaminar fracture toughness can be determined. The results have been summarized in Table 4. It is observed that the mode I translaminar fracture toughness of cotton/epoxy material is equal to $14.05~\text{MPa}\sqrt{\text{m}}$ and it is smaller than the mode II and III translaminar fracture toughness. As a result, the translaminar fracture toughness of the tested material is strongly dependent on the loading conditions.

4.3. Fracture envelopes

Some criteria have been proposed to investigate the mixed mode behavior of composite materials. Mixed-Mode Fracture Envelope (MMFE) is extensively used to evaluate the experimental data [41]. This criterion is written as follows:

$$\left(\frac{K_I}{K_{IC}}\right)^n + \left(\frac{K_{II}}{K_{IIC}}\right)^n + \left(\frac{K_{III}}{K_{IIIC}}\right)^0 = 1 \tag{11}$$

Fig. 12 illustrates the translaminar fracture envelope for the cotton/epoxy composites subjected to the different mixed mode loading conditions. It was obtained that the form of m=2 and n=1.8 is properly estimated the mixed mode I/II translaminar fracture behavior of the system (see Fig. 12a). Similar behavior was reported for the inter-laminar fracture toughness of the cotton/epoxy and some other laminated composites [29]. For the mixed mode I/III and II/III loading conditions, m, n and o were determined as 2, 1.8 and 1.8, respectively (see Fig. 12b and c).

4.4. Results comparison

The translaminar CSERR of cotton fiber reinforced epoxy-based laminated composites obtained in the current study have been compared with the translaminar CSERR of other systems in Table 5. It is well demonstrated that the translaminar CSERR of cotton/epoxy composites under pure fracture modes is remarkable as compared to the other laminated composite systems. The lower bound value of mode I translaminar CSERR of cotton/epoxy composites was obtained as 48.1 kJ/m².

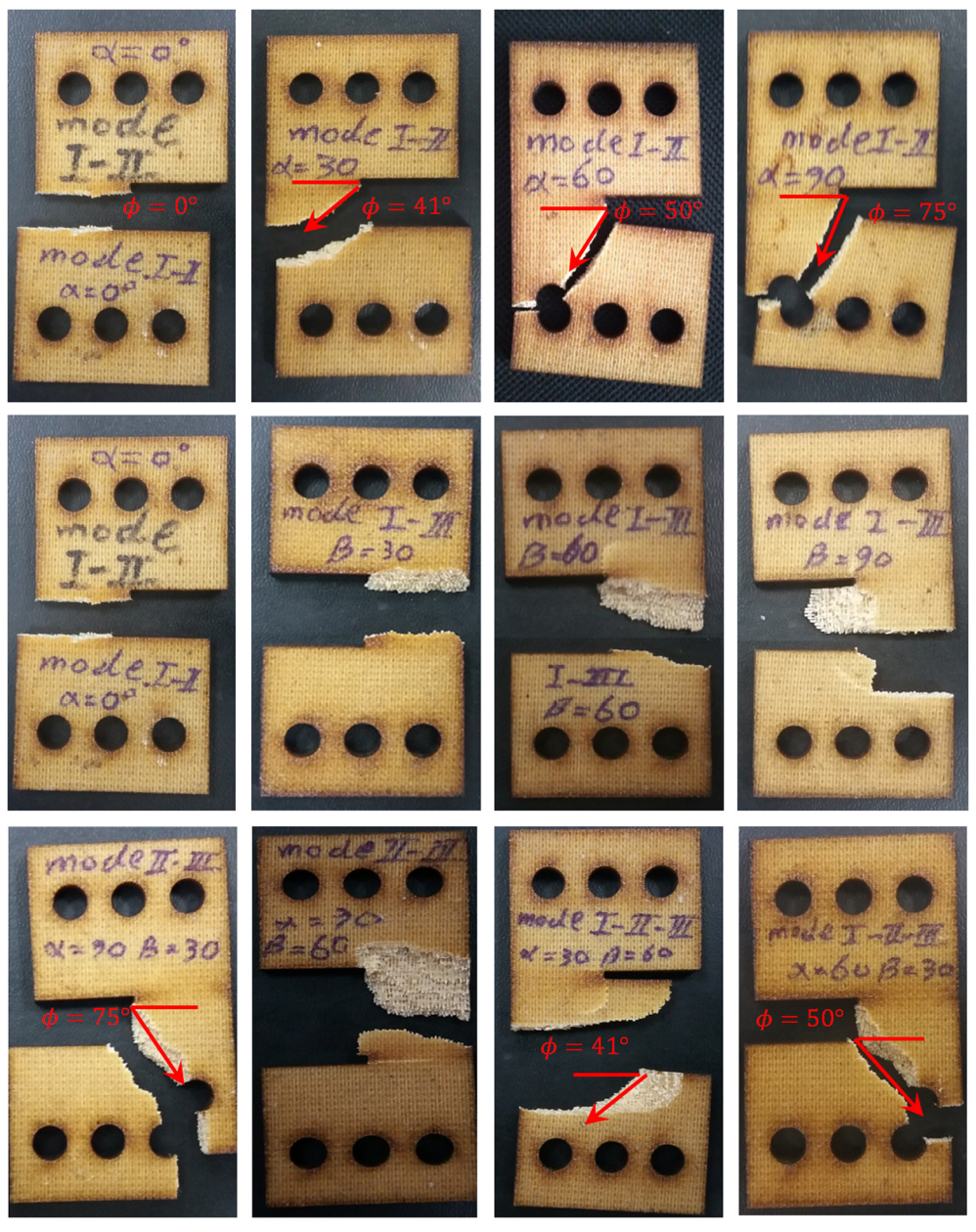


Fig. 13. Typical fracture profile of the CTS specimens made of cotton/epoxy system under different loading angles.

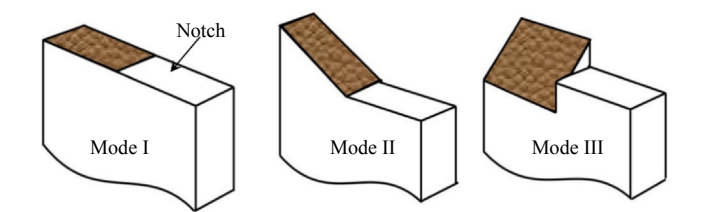


Fig. 14. Schematic of crack deflection of brittle materials under different loading conditions.

It is observed that the woven cotton/epoxy system has a significant value of mode I translaminar CSERR as compared to the woven glass/epoxy [18,42], woven carbon/epoxy [42], unidirectional carbon/epoxy [11,35,43,44]. Besides, the mode I translaminar fracture toughness of the cotton fiber reinforced composites has been compared with the pure epoxy. It was tabulated in Table 2 that the lower bound value of mixed mode I/II translaminar CSERR of the tested composite is around

 $300~kJ/m^2$. Whereas, Laffan et al. [11] obtained a value of $11~kJ/m^2$ for the mixed mode I/II translaminar CSERR of the unidirectional carbon/epoxy system.

In Ref. [5], the inter-laminar CSERR and fracture toughness of the cotton/epoxy system under mixed mode I/II/III loading condition have been reported. Table 6 compares the inter-laminar and translaminar fracture responses of this material. It is well observed that the crack direction has a strong effect on the fracture response of the cotton/epoxy material. According to Table 6, by increasing the mode III contribution, both inter-laminar and translaminar fracture toughness values are significantly increased.

4.5. Crack growth direction

The crack growth direction is one of the main reasons that lead to increase the mode II CSERR of the sample in comparison with the mode I loading state [29,45]. Hence, this section investigates the crack growth direction of CTS samples tested under different loading angles.

A protractor was used in order to measure the observed crack propagation angle of the cotton/epoxy system. The arrows in Fig. 13 indicate the crack propagation direction for the fractured specimens. For mixed mode I/II loading condition, it is clearly shown that the magnitude of crack deflection angle increases for the higher contribution of mode II fracture. It is also concluded that in the presence of mode III fracture, the fracture surface is remarkably enhanced as compared to the other loading conditions.

As the crack deflection in the cotton/epoxy CTS samples compared to the brittle fracture in materials such as pure epoxy [29] (see Fig. 14), the translaminar fracture in cotton/epoxy system has brittle behavior. This behavior can be proved by the load–displacement curve observed in Section 2.3. Besides, the curves for mixed mode I/II fracture of cotton/epoxy material show a semi brittle behavior (see Fig. 8).

5. Conclusion

In this work, a combined practical study and FE analysis was performed in order to characterize the mixed mode I/II/III translaminar CSERR of cotton fiber reinforced laminated composites. The laminated composites samples were loaded by Arcan and out-of-plane fixtures. The translaminar CSERR of the natural laminated composites under a full range of mixed mode I/II/III loading conditions was calculated. Some important results can be expressed as follows:

- The results manifested that the translaminar CSERR of cotton/epoxy laminates are remarkably affected by the mode mixity.
- The lowest and highest translaminar fracture toughness values are related to the mode I and mixed mode II/III fracture tests, respectively.
- Under mixed mode I/III loading, by increasing the mode III contribution translaminar fracture, the value of CSERR is also increased.
- The criterion of Mixed-Mode Fracture Envelope was used to predict the mixed mode I/II/III translaminar fracture behavior of cotton/ epoxy system. An appropriate relation was obtained in this case.
- As a result, the crack deflection of cotton/epoxy system is similar to the brittle materials.
- The mode I translaminar CSERR of cotton/epoxy laminates is remarkable as compared to the mode I translaminar CSERR of the other systems. Thus, in the presence of an out-of-plane crack in a sheet, the cotton fiber reinforced composites can be utilized.
- It must be noted that in order to design and simulate a structure, the values such as translaminar CSERR and fracture toughness are required to be determined. Hence, the results of this study are usable when the simulation of a structure is necessary to be performed.

Declaration of Competing Interest

The authors declare that they have no known competing financial interests or personal relationships that could have appeared to influence the work reported in this paper.

References

- P. Wambua, J. Ivens, I. Verpoest, Natural fibres: can they replace glass in fibre reinforced plastics, Compos. Sci. Technol. 63 (9) (2003) 1259–1264, https://doi. org/10.1016/S0266-3538(03)00096-4.
- [2] M.C. Khoathane, O.C. Vorster, E.R. Sadiku, Hemp fiber reinforced 1-pentene/ polypropylene copolymer: The effect of fiber loading on the mechanical and thermal characteristics of the composites, J. Reinf. Plast. Compos. 27 (14) (2008) 1533–1544, https://doi.org/10.1177/0731684407086325.
- [3] S. Keck, M. Fulland, Effect of fibre volume fraction and fibre direction on crack paths in unidirectional flax fibre-reinforced epoxy composites under static loading, Theor. Appl. Fract. Mech. 101 (2019) 162–168, https://doi.org/10.1016/j.tafmec. 2019.01.028
- [4] H. Ku, H. Wang, N. Pattarachaiyakoop, N. Trada, A review on the tensile properties of natural fiber reinforced polymer composites, Compos. Part B. Eng. 42 (4) (2011) 856–873, https://doi.org/10.1016/j.compositesb.2011.01.010.
- [5] E. Moradi, A. Zeinedini, On the mixed mode I/II/III inter-laminar fracture

- toughness of cotton/epoxy laminated composites, Theor. Appl. Fract. Mech. (2019) 102400, https://doi.org/10.1016/j.tafmec.2019.102400.
- [6] M.M. Shokrieh, A. Zeinedini, S.M. Ghoreishi, On the mixed mode I/II delamination R-curve of E-glass/epoxy laminated composites, Compos. Struct. 171 (2017) 19–31, https://doi.org/10.1016/j.compstruct.2017.03.017.
- [7] M.J. Laffan, S.T. Pinho, P. Robinson, A.J. McMillan, Translaminar fracture toughness testing of composites: A review, Polym. Test. 31 (2012) 481–489, https://doi.org/10.1016/j.polymertesting.2012.01.002.
- [8] J.H. Underwood, M.T. Kortschot, Notch-tip Damage and Translaminar Fracture Toughness Measurements from Carbon/Epoxy Laminates, US Army Armament Research Development and Engineering Centre, 1994 Technical Report ARCCB-TR-94010.
- [9] M.J. Laffan, S.T. Pinho, P. Robinson, A.J. McMillan, Translaminar fracture toughness: the critical notch tip radius of 0-plies in CFRP, Compos. Sci. Technol. 72 (2011) 97–102, https://doi.org/10.1016/j.compscitech.2011.10.006.
- [10] L. Gigliottiand, S.T. Pinho, Translaminar fracture toughness of NCF composites with multiaxial blankets, Mater. Des. 94 (2016) 410–416, https://doi.org/10.1016/j. matdes.2015.12.167.
- [11] M.J. Laffan, S.T. Pinho, P. Robinson, Mixed-mode translaminar fracture of CFRP: Failure analysis and fractography, Compos. Struct. 95 (2013) 135–141, https://doi. org/10.1016/j.compstruct.2012.06.012.
- [12] R.F. Teixeira, S.T. Pinho, P. Robinson, Thickness-dependence of the translaminar fracture toughness: experimental study using thin-ply composites, Compos. Part A Appl. Sci. Manuf. 90 (2016) 33–44, https://doi.org/10.1016/j.compositesa.2016. 05.031.
- [13] M. Chabchoub, D. Bouscarrat, B. Vieille, C. Gautrelet, M. Beyaoui, M. Taktak, M. Haddar, L. Taleb, Investigations on the mode I translaminar failure and determination of fracture toughness in woven-ply carbon fibers thermoplastic composites at high temperatures, Appl. Acoust. 128 (2017) 55–63, https://doi.org/10. 1016/j.apacoust.2017.01.028.
- [14] X. Xu, A. Paul, M.R. Wisnom, Thickness effect on mode I trans-laminar fracture toughness of quasi-isotropic carbon/epoxy laminates, Compos. Struct. 210 (2019) 145–151, https://doi.org/10.1016/j.compstruct.2018.11.045.
- [15] G. Bullegas, T.S. Pinho, S. Pimenta, Engineering the translaminar fracture behaviour of thin-ply composites, Compos. Sci. Technol. 131 (2016) 110–122, https://doi.org/10.1016/j.compscitech.2016.06.002.
- [16] L. Marín, E.V. Gonz_alez, P. Maimí, D. Trias, P.P. Camanho, Hygrothermal effects on the translaminar fracture toughness of cross ply carbon/epoxy laminates: Failure mechanisms, Compos. Sci. Technol. 122 (2016) 1301–2139, https://doi.org/10. 1016/j.compscitech.2015.10.020.
- [17] S. Jose, R. Ramesh Kumar, M.K. Jana, G. Venkateswara Rao, Intralaminar fracture toughness of a cross-ply laminate and its constituent sub-laminates, Compos. Sci. Technol. 61 (2001) 1115–1122, https://doi.org/10.1016/S0266-3538(01)00011-2.
- [18] D. Boyina, A. Banerjee, R. Velmurugan, Mixed-mode translaminar fracture of plain-weave composites, Compos. Part B. Eng. 60 (2014) 21–28, https://doi.org/10.1016/j.compositesb.2013.12.052.
- [19] J. Jamali, M.J. Mahmoodi, M.K. Hassanzadeh-Aghdam, J.T. Wood, A mechanistic criterion for the mixed-mode fracture of unidirectional polymer matrix composites, Compos. Part B Eng. 176 (2019) 107316, https://doi.org/10.1016/j.compositesb. 2019 107316
- [20] K.V. Arun, S. Basavarajappa, C. Chandrakumar, S.M. Yadav, Influence of secondary fillers on the behavior of translaminar failure in glass-epoxy composites, Polym. Plast. Technol. Eng. 49 (5) (2010) 495–502, https://doi.org/10.1080/ 02560255002412020
- [21] T. Lisle, M.L. Pastor, C. Bouvet, P. Marguerès, Damage of woven composite under translaminar cracking tests using infrared thermography, Compos. Struct. 161 (2017) 275–286, https://doi.org/10.1016/j.compstruct.2016.11.030.
- [22] K.V. Arun, R.D. Kamat, S. Basavarajappa, Mechanism of translaminar fracture in glass/textile fabric polymer hybrid composites, J. Reinf. Plast. Compos. 29 (2) (2008) 254–265, https://doi.org/10.1177/0731684408097759.
- [23] R. Haj-Ali, R. El-Hajjar, Crack propagation analysis of mode-I fracture in pultruded composites using micromechanical constitutive models, Mech. Mater. 35 (2003) 885–902, https://doi.org/10.1016/S0167-6636(02)00290-9.
- [24] F. Hou, S. Hong, Characterization of R-curve behavior of translaminar crack growth in cross-ply composite laminates using digital image correlation, Eng. Fract. Mech. 117 (2014) 51–70, https://doi.org/10.1016/j.engfracmech.2014.01.010.
- [25] S.I.B. Syed Abdullah, L. Iannucci, E.S. Greenhalgh, On the translaminar fracture toughness of Vectran/epoxy composite material, Compos. Struct. 202 (2018) 566–577, https://doi.org/10.1016/j.compstruct.2018.03.004.
- [26] Q. Liu, M. Hughes, The fracture behaviour and toughness of woven flax fibre reinforced epoxy composites, Compos. Part A Appl. Sci. Manuf. 39 (2008) 1644–1652, https://doi.org/10.1016/j.compositesa.2008.07.008.
- [27] M.R.M. Aliha, S.S. Mousavi, A. Bahmani, E. Linul, L. Marsavina, Crack initiation angles and propagation paths in polyurethane foams under mixed modes I/II and I/ III loading, Theo. Appl. Fract. Mech. 101 (2019) 152–161, https://doi.org/10. 1016/j.tafmec.2019.02.016.
- [28] ASTM E1922, Standard Test Method for Translaminar Fracture Toughness of Laminated and Pultruded Polymer Matrix Composite Materials, ASTM International, Philadelphia, 2015.
- [29] A. Zeinedini, A novel fixture for mixed mode I/II/III fracture testing of brittle materials, Fatigue Fract. Eng. Mater. Struct. (2018) 1–16, https://doi.org/10.1111/ ffe.12955.
- [30] ASTM D3039, Standard Test Method for Tensile Properties of Polymer Matrix Composite Materials, ASTM International, Philadelphia, 2002.
- [31] ASTM D3518, Standard Test Method for In-Plane Shear Response of Polymer Matrix Composite Materials by Tensile Test of a 45° Laminate, ASTM International,

- Philadelphia, 2001.
- [32] ASTM D790, Standard Test Methods for Flexural Properties of Unreinforced and Reinforced Plastics and Electrical Insulating Materials, ASTM International, Philadelphia, 2003.
- [33] N. Choupani, Experimental and numerical investigation of the mixed-mode delamination in Arcan laminated specimens, Mater. Sci. Eng. A 478 (1–2) (2008) 229–242, https://doi.org/10.1016/j.msea.2007.05.103.
- [34] H. Chyanbin, J.S. Hu, Stress intensity factors and energy release rates of delaminations in composite laminates, Eng. Fract. Mech. 42 (6) (1992) 977–988, https://doi.org/10.1016/0013-7944(92)90137-4.
- [35] S.T. Pinho, P. Robinson, L. Iannucci, Fracture toughness of the tensile and compressive fibre failure modes in laminated composites, Compos. Sci. Technol. 66 (2006) 2069–2079, https://doi.org/10.1016/j.compscitech.2005.12.023.
- [36] M.M. Shokrieh, M. Heidari-Rarani, Effect of stacking sequence on R-curve behavior of glass/epoxy DCB laminates with 0°//0° crack interface, Mater. Sci. Eng. A. 529 (2011) 265–269, https://doi.org/10.1016/j.msea.2011.09.027.
- [37] ASTM D5528-13, Standard Test Method for Mode I Interlaminar Fracture Toughness of Unidirectional Fiber-Reinforced Polymer Matrix Composites, ASTM International, Philadelphia, 2013.
- [38] ASTM D6671/D6671M-19, Standard Test Method for Mixed Mode I-Mode II Interlaminar Fracture Toughness of Unidirectional Fiber Reinforced Polymer Matrix Composites, ASTM International, Philadelphia, 2019.
- [39] ASTM D7905/D7905M-19e1, Standard Test Method for Determination of the Mode II Interlaminar Fracture Toughness of Unidirectional Fiber-Reinforced Polymer

- Matrix Composites, ASTM International, Philadelphia, 2019.
- [40] M.M. Shokrieh, M. Heidari-Rarani, S. Rahimi, Influence of curved delamination front on toughness of multidirectional DCB specimens, Compos. Struct. 94 (4) (2012) 1359–1365, https://doi.org/10.1016/j.compstruct.2011.11.035.
- [41] S.A. Jones, R.A. Tomlinson, Investigating mixed-mode (I/II) fracture in epoxies using digital image correlation: Composite G_{IIc} performance from resin measurements, Eng. Fract. Mech. 149 (2015) 368–374, https://doi.org/10.1016/j. engfracmech.2015.08.041.
- [42] D. Dalli, G. Catalanotti, L.F. Varandas, B.G. Falzon, S. Foster, Mode I intralaminar fracture toughness of 2D woven carbon fibre reinforced composites: A comparison of stable and unstable crack propagation techniques, Eng. Fract. Mech. 214 (2019) 427–448, https://doi.org/10.1016/j.engfracmech.2019.04.003.
- [43] M.J. Laffan, S.T. Pinho, P. Robinson, L. Iannucci, Measurement of the in situ ply fracture toughness associated with mode I fibre tensile failure in FRP, Part I: data reduction, Compos. Sci. Technol. 70 (2010) 606–613, https://doi.org/10.1016/j. compscitech.2009.12.016.
- [44] G. Catalanotti, P.P. Camanho, J. Xavier, C.G. Dávila, A.T. Marques, Measurement of resistance curves in the longitudinal failure of composites using digital image correlation, Compos. Sci. Technol. 70 (2010) 1986–1993, https://doi.org/10.1016/j. compscitech.2010.07.022.
- [45] J. Jamali, Y. Fan, J.T. Wood, The mixed-mode fracture behavior of epoxy by the compact tension shear test, Int. J. Adhes. Adhes. 63 (2015) 79–86, https://doi.org/ 10.1016/j.ijadhadh.2015.08.006.